Adv Biochem Engin/Biotechnol (2011) 124: 55–81
DOI: 10.1007/10_2010_97

Published Online: 12 November 2010

Algebraic and Geometric Understanding of Cells: Epigenetic Inheritance of Phenotypes Between Generations

Kenji Yasuda

Abstract We have developed methods and systems for analyzing epigenetic information in cells, as well as that of genetic information, to expand our understanding of how living systems are determined. Because cells are minimum units reflecting epigenetic information, which is considered to map the history of a parallel-processing recurrent network of biochemical reactions, their behaviors cannot be explained by considering only conventional DNA information-processing events. The role of epigenetic information in cells, which complements their genetic information, was inferred by comparing predictions from genetic information with cell behavior observed under conditions chosen to reveal adaptation processes and community effects. A system for analyzing epigenetic information was developed starting from the twin complementary viewpoints of cell regulation as an 'algebraic' system (emphasis on temporal aspects) and as a 'geometric' system (emphasis on spatial aspects). The knowledge acquired from this study may lead to the use of cells that fully control practical applications like cell-based drug screening and the regeneration of organs.

Keywords On-chip single-cell-based cultivation/analysis · Epigenetic information · Algebraic viewpoint · Geometric viewpoint · Individuality

Contents

K. Yasuda (✉)
Department of Biomedical Information, Institute of Biomaterials and Bioengineering, Tokyo Medical and Dental University, 2-3-10 Kanda-Surugadai, Chiyoda-ku, Tokyo 101-0062, Japan
e-mail: yasuda.bmi@tmd.ac.jp

1 Introduction: On-Chip Cultivation Methods for 'Algebraic' and 'Geometric' Viewpoints

Cells are minimum units determining their responses through genetic and epigenetic information like the history of interactions between them and fluctuations in environmental conditions affecting them. The cells in a group are also individual entities, and their differences arise even among cells with identical genetic information that have grown under the same conditions. These cells respond differently to perturbations [1]. Why and how do these differences arise? To understand the rules underlying possible differences occurring in cells, we need to develop methods of simultaneously evaluating both the genetic and epigenetic information not only for molecular level measurement but also for functional measurement. In other words, if we are to understand topics like variations in cells with the same genetic information, inheritance of non-genetic information between adjacent generations of cells, cellular adaptation processes caused by environmental change, the community effect of cells, we also need to analyze their epigenetic information. We thus started a series of studies to analyze epigenetic information among neighboring generations of cells and in the spatial structures of cell network to expand our understanding of how the fates of living systems are determined. As cells are minimum units reflecting epigenetic information, which is considered to map the history of a parallel-processing recurrent network of biochemical reactions, their behaviors cannot be explained by considering only conventional DNA information-processing events. The role of epigenetic information in the higher complexity of cellular groups, which complements their genetic information, is inferred by comparing predictions from genetic information with cell behavior observed under conditions chosen to reveal adaptation processes and community effects. A system for analyzing epigenetic information should be developed starting from the twin complementary viewpoints of cell regulation as an 'algebraic' system (emphasis on temporal aspects; adaptation among generations) and as a 'geometric' system (emphasis on spatial aspects; spatial pattern-dependent community effect). The acquired knowledge should lead us not only to understand the mechanism of the inheritable epigenetic memory but also to be able to control the epigenetic information by the designed sequence of the external stimulation.

As we can see in Fig. 1, the strategy behind our on-chip microfabrication method is constructive, involving three steps. First, we purify cells from tissue one

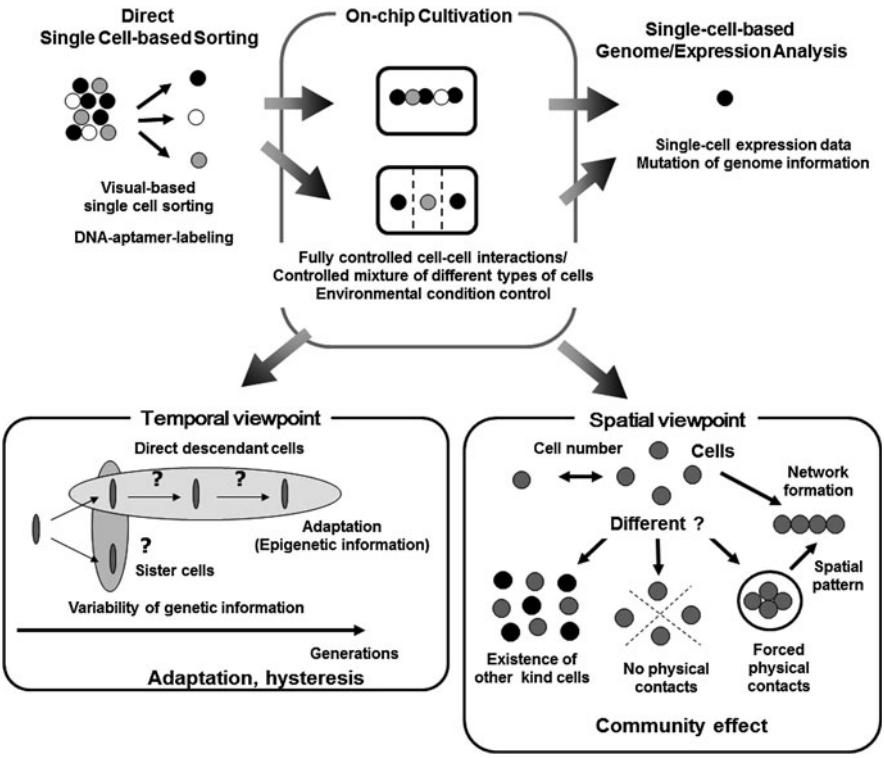

Fig. 1 Our strategy: on-chip single-cell-based analysis with the aim of probing temporal and spatial aspects of cell regulation

by one in a nondestructive manner such as using ultrahigh-speed camera-based real-time cell sorting, or digestible DNA-aptamer labeling [2]. We then cultivate and observe them under fully controlled conditions (e.g., cell population, network patterns, or nutrient conditions) using an on-chip single-cell cultivation chip [3–12] or an on-chip agarose microchamber system [13–20]. Finally, we perform single-cell-based genome/proteome analysis through photothermal denaturation and single-molecule level analysis [21].

In this chapter, we explain the aims of our single-cell-based study using the single-cell-based cultivation/analysis system and introduce some of the results focusing on the 'algebraic' understanding of cellular systems using *Escherichiacoli* cells.

2 Cultivation System for 'Algebraic' Viewpoint: On-Chip Single-Cell Cultivation System for Isolated *E. coli* Cells

The first aim of our single-cell-based study was to develop methods and systems using on-chip microcultivation system that enable the mechanism responsible for

controlling (regulating) cells epigenetically to be analyzed for 'algebraic' understanding. The advantage of this approach is that it removes the complexity in underlying physicochemical reactions that are not always completely understood and for which most of the necessary variables cannot be measured. Moreover, this approach shifts the view of cell regulatory processes from a basic chemical ground to a paradigm of the cell as an information-processing unit working as an intelligent machine capable of adapting to changing environmental and internal conditions. This is an alternative representation of the cell and can bring new insights into cellular processes. Thus, models derived from such a viewpoint can directly help in more traditional biochemical and molecular biological analyses that assist in our understanding of control in cells.

Phenotypic and behavioral variations from cell to cell have been observed to exist even in a genetically identical population [1, 22–25]. The resulting heterogeneity in a clonal population may well be important not only for survival [24], but also for cooperation in a population that must obviously exist and work in multicellular organisms [26–28]. The mechanisms of producing phenotypic variations are explored both theoretically [29–34] and experimentally [35–37] as an intracellular noise (fluctuation, or stochastic transcription/translation)-driven process [38]. McAdams and Arkin proposed that stochasticity in the process of gene expression could lead to the substantially large difference in the amount of protein products, which eventually affects the switching mechanisms in individual cells in a group that select between alternative phenotypes [33]. The existence of noise in the gene expression process was shown experimentally by van Oudenaarden and colleagues [37]. They showed that the resulting phenotypic noise had a strong positive correlation with translational efficiency, in contrast to the weak positive correlation observed for transcriptional efficiency. As another example of the experiment, Elowitz and colleagues [36] examined the contributions to overall variation from the gene expression process and from other cellular components separately, showing that the noise in the gene expression process did not uniquely determine the total variability.

These studies are based on the temporal observation of a cell group. The group-based observation, however, cannot show how an individual cell produces different phenotypes and behaviors in the course of proliferation and whether phenotypes and behaviors specific to an individual cell can be inherited. Flow cytometry enables us to obtain the distributions of parameters like concentration, size, shape, DNA content etc. at the single-cell level in a group and is a powerful method to check huge numbers of cells within a short time [39]. To confirm the acquired results from flow cytometry, as a complementary supporting approach, it is desirable to acquire the continuous trackings of a specific single cell's dynamics under the specific circumstances like isolated conditions or comparison of neighboring generations of single cells. In other words, cytometry can give us information about the average properties of huge numbers of cells, i.e., how the group changes, but it cannot give us information about how a single cell changes. Direct microscopic measurement of cells in solid media like cultivation plates [28, 40–43] can identify individual cells and thus can track specific cells continuously.

Although we can begin cultivating cells under isolated conditions and establish the desired connections by controlling the initial spread concentration, it is impossible to keep cells isolated or track more than ten direct descendant generations especially after cell divisions have occurred, and it is impossible to control the interactions between particular cells because the positions of the cells are fixed at the beginning of the cultivation. Thus this on-chip measurement system is thought to be complementary to these conventional methods for gaining an understanding of single-cell level interactions of particular cells.

New techniques are needed to clarify the interactions between genetically identical cells, and for this purpose, we have developed an on-chip single-cell-based microculture method exploiting recent microfabrication techniques and conventional in vivo techniques. To manipulate cells in microchambers, we use non-contact forces, such as optical tweezers and acoustic radiation force, which have been used to handle cells, organelles, and biomolecules on microscope specimens [2, 44–49].

2.1 On-Chip Single-Cell Cultivation System Design

To directly compare sister or direct descendant cells, we developed an on-chip single-cell cultivation system. It enabled excess cells to be transferred from the analysis chamber to the waste chamber through a narrow channel that allowed a particular cell to be selected from cells in the microfabricated cultivation chamber with non-contact force, optical tweezers (Fig. 2).

Figure 3 is a schematic drawing of the procedure of isolation of single cells using optical tweezers, and the entire system we used for on-chip single-cell-based

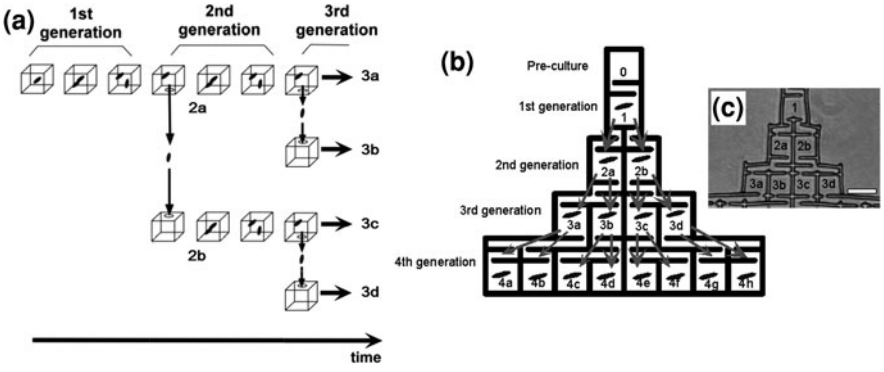

Fig. 2 Single-cell cultivation in microchambers to measure variability in genetic information. **a** Schematic drawing of concept of on-chip single cell cultivation using microchamber system, **b** an example of microchamber array design for single cell cultivation for four generations, **c** micrograph of microchamber array structure made of polydimethylsiloxane (PDMS) on the glass slide, *bar* 50 μm

analysis. It consists of a microchamber array plate (chip), a cover chamber attached to the medium circulation unit, a ×100 phase-contrast/fluorescent microscope, and optical tweezers. The microchamber arrays are the microfabricated structure etched on the glass slide (Fig. 4a–e), or made of thick photo-resist SU-8-5 on the glass slide (Microlithography Chemical Corp., MA) (Fig. 4f). The height of the microchamber array is at least 5 μm, in which the cells are enclosed. The microchamber array is sealed with a semipermeable membrane to prevent the cells escaping from it. The semipermeable membrane is decorated with avidin and the glass slide with biotin to ensure the seal is tight (Fig. 5). With these decorations on the membrane and slide, it is possible to observe cells in the microchamber without them escaping. The microchamber is composed of two main parts and the first is the observation area, which has four compartments in it at the center of the microchamber. Each compartment has a volume of 20 × 20 × 5 μm. Each compartment has four observation sub-compartments (A, B, C, and D in Fig. 4f) at the center of the microstructure. The second part includes the discarding areas at both sides of the microchamber. These enclose surplus cells in observations. The first four direct descendant cells derived from a single cell were placed in one of the four compartments individually to keep them isolated. The excess descendant cells were transferred to the two large compartments (discarding areas) along the white arrow with the optical tweezers. Cells were transferred from the observation area to the discarding area by using the optical tweezers through the narrow path along the white arrow in Fig. 4f. As we can see in the micrographs, only one cell is enclosed in each of the four compartments of the observation area

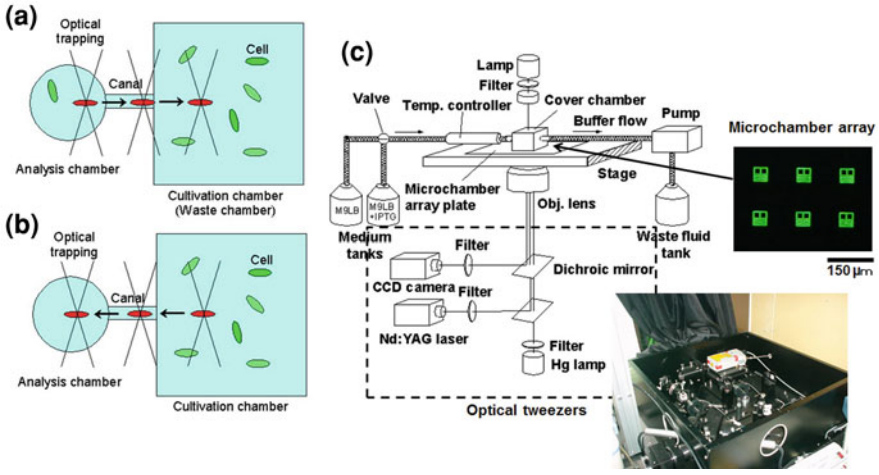

Fig. 3 On-chip single-cell cultivation system for *E. coli* cells. **a** One of the divided two daughter cells was removed from analysis chamber, **b** one of the cultivated cells in a group in the cultivation chamber was picked up and transferred into the analysis chamber, **c** schematic drawing and micrographs of the system

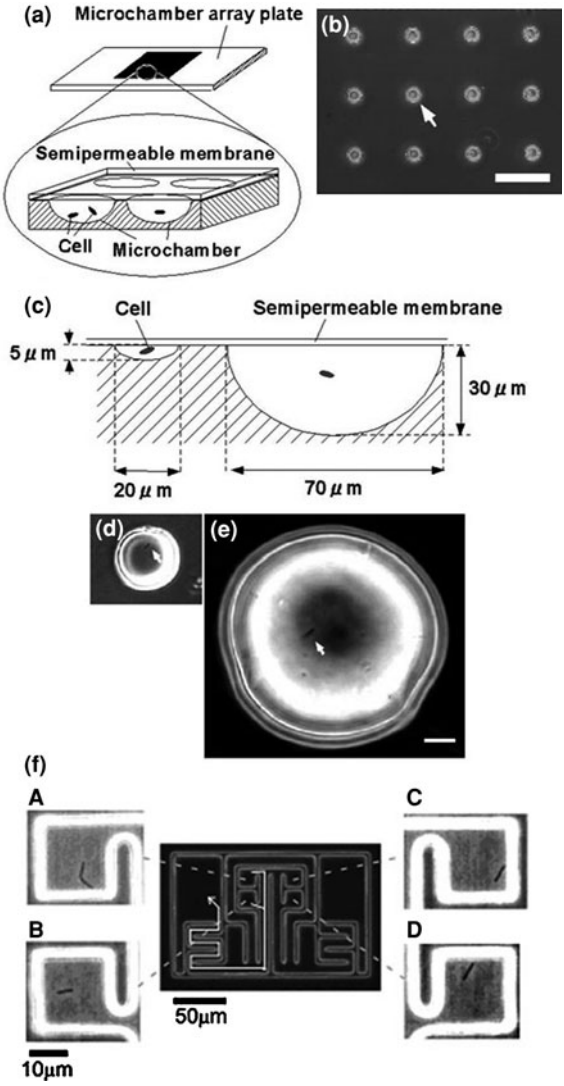

Fig. 4 Optical micrographs of microchambers. **a** Schematic drawing of the microchamber array plate. An $n \times n$ ($n = 20$–50) array of microchambers is etched into a 0.17-mm-thick glass slide. Each microchamber is covered with a semipermeable membrane separating the chamber from the nutrient medium circulating through the medium bath. A single cell or group of cells in the microchamber can thus be isolated from others perfused with the same medium. **b** Optical micrograph of the microchamber array plate. The *arrow* indicates the position of one microchamber with a 20-μm diameter and 5-μm depth. *Bar* 100 μm. **c** Schematic drawing of the two sizes of microchambers. The 'small chamber' on the *left* has a 20-μm diameter and 5-μm depth (shown in **b**), and the 'large chamber' on the *right* has a 70-μm diameter and 30-μm depth. Optical micrographs of **d** a small chamber, and **e** a large chamber. The *arrows* indicate the positions of *E. coli* in the chambers. *Bar* 10 μm. **f** Microchamber array with four compartments

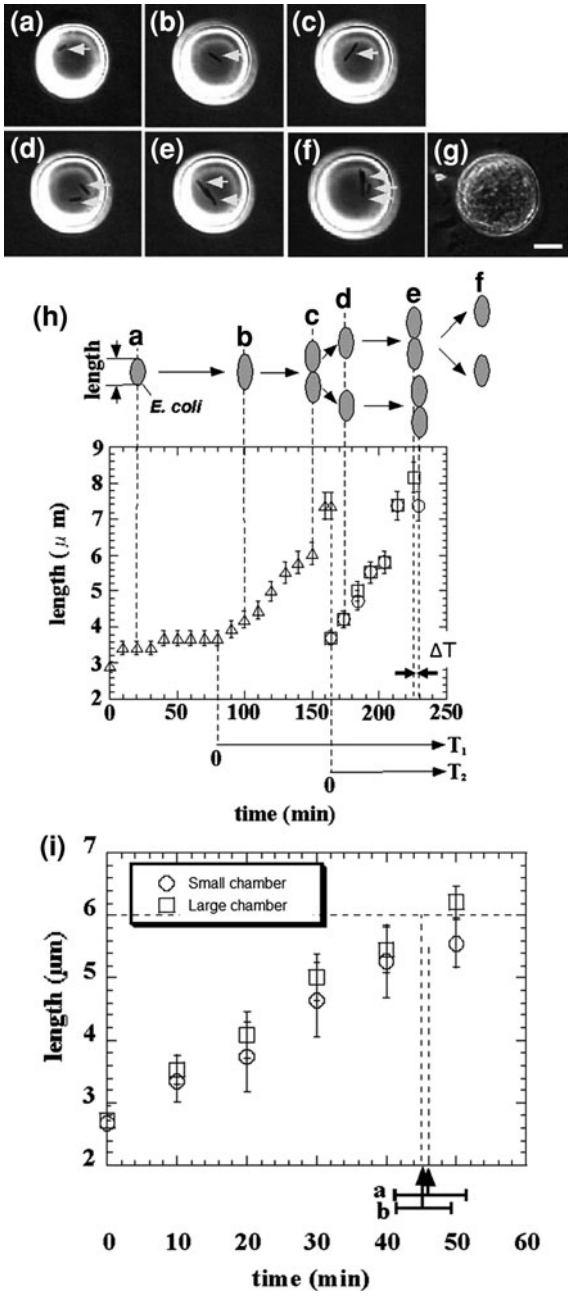

Fig. 5 Differential analysis of sister cells from isolated single *E. coli* in a micro-chamber. The magnified micrographs at the top **a**–**g** show the time course of one of the microchambers in Fig. 4b (see *arrow*) at times of **a** 0 min, **b** 100 min, **c** 150 min, **d** 175 min, **e** 225 min, **f** 230 min, and **g** 15 h after the inoculation started. The *arrows* in the micrographs show the positions of *E. coli* in the microchamber. *Bar* 10 μm. **h** Time course growth of the individual *E. coli*. **i** Chamber size dependence of cell growth and interdivision time, small chamber and large chamber in Fig. 4c (*open circle* and *open square* for cell length, and *a* and *b* for interdivision time, respectively), indicating no dependence of cell growth speed on chamber size

under isolated conditions. Four specific cells in the four compartments were simultaneously observed without any disruption by the other cells and without leaving the field of view of the microscope.

Optical tweezers were introduced to enable non-contact handling of the cell specimens. An Nd:YAG laser (wavelength = 1,064 nm, T20-8S, Spectra Physics, SpectraPhysics, CA) was guided to the ×100 phase contrast objective lens (UplanApo, Olympus, Tokyo, Japan) as the light source for the optical tweezers, which are widely used in handling micron-sized particles and biomaterials [44–49]. We used it in the system in our protocol to transport particular cells within the microchamber.

The medium circulation unit utilized a glass box with a volume of 1 ml that had two branches. It was mounted on the microchamber array chip and fresh medium buffer was always circulated in the glass box through the two branches at a rate of 1 ml/min with a peristaltic pump. The bottom of the glass box was open and the condition of the medium around the cells could be constantly maintained by buffer exchanges through the semipermeable membrane.

A phase contrast microscope (obj. ×100 magnitude) was set up with IX-70 (Olympus). The whole microcultivation part was placed in a thermo control cage (IX-IBM, Olympus) to maintain the temperature at 37 °C throughout observation. The observation images were taken with a CCD camera (CS230, Olympus) and recorded on digital video cassette. These were analyzed on a personal computer (PCV-R73 K, Sony, Tokyo, Japan).

2.2 *Differential Analysis of Sister Cells with Identical Genetic Information and Experience*

To investigate non-genetic variability in the division cycle and growth of single cells, we first compared the growth and division times for pairs of *E. coli* daughter cells under isolated conditions using the on-chip single-cell cultivation system we just have described [3, 5] (Figs. 3 and 4).

In this experiment, we used *E. coli* strain JM109 (*end*A1, *rec*A1, *gyr*A96, *thi*, *hsd*R17(r_k^-, m_k^+), *rel*A1, *sup*E44, λ^-, Δ(*lac-pro*AB), [F′, *tra*D36, *pro*AB, *lac*$I^qZ\Delta M15$] obtained from Toyobo, Tokyo, Japan) in a minimal medium, M9 (4.5 g/l KH_2PO_4, 10.5 g/l K_2HPO_4, 50 mg/l $MgSO_4 \cdot 7H_2O$, pH 7.1) containing 0.2% (w/w) of glucose at 37 °C.

First, we checked the chamber size dependence of cell growth and interdivision time using different sized microchambers (Fig. 4c) and found there no apparent difference (Fig. 5i).

Before starting continuous isolation of direct descendant cells using optical tweezers, we have compared the difference of growth and divisions of sister cells within the microchambers under the conditions without any physical stimulation applied to the cultivating cells. After on-chip single-cell cultivation has started, an isolated single cell (mother cell) grew in the microchamber after the resting of growth from 2.8 to 5.6 μm in 90 min, and finally divided into two 2.8-μm daughter cells (Fig. 6a). Although the newborn daughter cells grew synchronously in the same manner, they divided into granddaughter cells at different times, i.e., 70 and

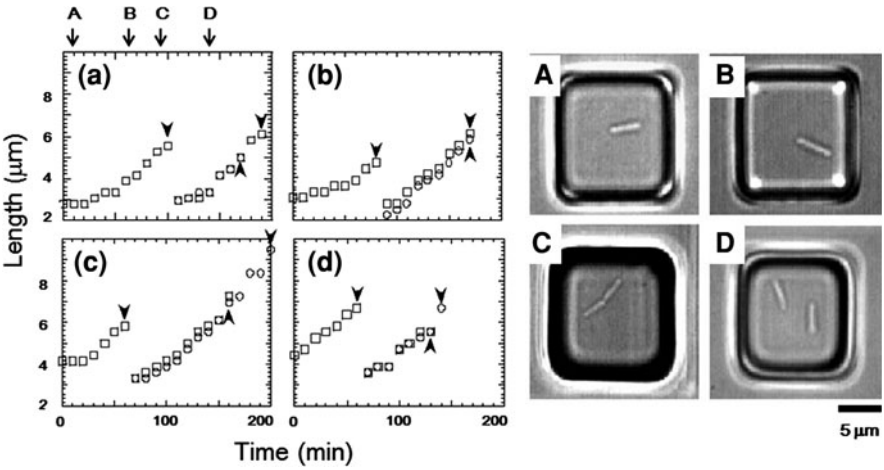

Fig. 6 Time course growth for isolated individual *E. coli* and two daughters

90 min (see arrowheads in graph). The three other examples (Fig. 6b–d) show that even though the growth of the mother cell and her daughter cells seems to have no significant correlation, the growth of two daughter cells from the same mother cell seems to be quite similar. In contrast, the division times for daughter cells of the same length (Fig. 6a, c, d) were not synchronous. In Fig. 6b, on the other hand, the division time and cell growth tendency of two daughter cells were synchronous even though they were born after unequal divisions of the mother cell. These results indicate that variations in cell growth and cell division may not be closely correlated and that cell division time is independent of genetic identity and cell size.

The division time differences between two daughter cells from the same mother cells were also measured (Fig. 7). Although sister cells are thought to have the same DNA and chemical components as their mother's cells, the results revealed only 36% of daughter cells divided into granddaughter cells within a 10-min difference of period even when they started at the same cell lengths (Fig. 7a). The dependence of division time differences for newborn daughter cells on length was also evaluated and the time distribution was similar regardless of the initial length (Fig. 7b). These results mean that variations in cell division may not depend on DNA or the initial cell size.

The initial dependence of variations in cell growth and division on length was also evaluated. The ratio of the final length of these cells and their initial length seems to be independent of the initial length, about 170%, when it is longer than 3 μm. The speed of growth of cells also has no significant dependence on the initial length.

In this experiment, we observed and compared the cell growth and division of two daughter cells of isolated single *E. coli* using the on-chip culture system, and found a broad range of variations in cell growth and division time. Such variations are not attributable to the genetic differences in DNA. The variations in the growth

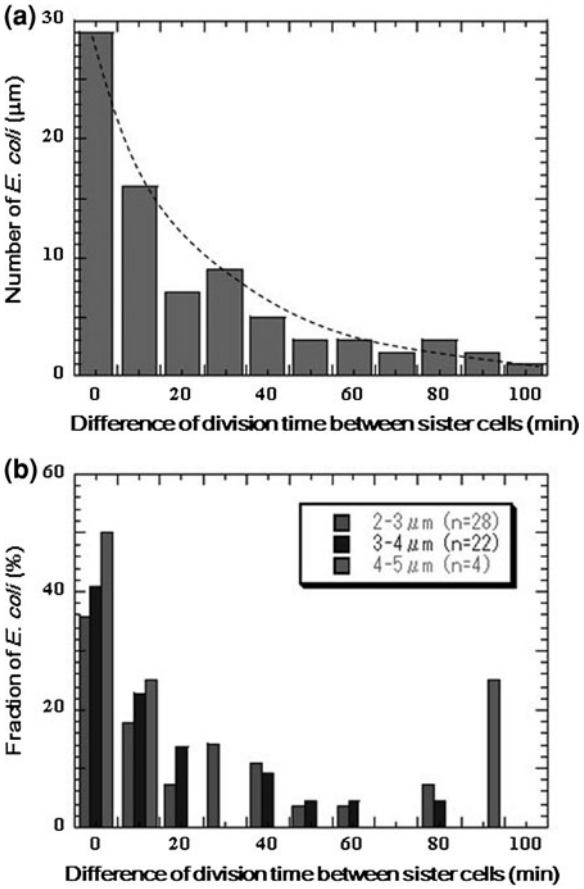

Fig. 7 **a** Differences in division time for two daughter cells of same mother cells ($n = 80$ pairs), and **b** initial dependence of division time differences on length

ratio between the final and initial lengths, and the speed of growth seem to be independent of their initial length, at least when they are longer than 3 μm. The same tendency toward a broad distribution in the division time (data not shown) and the division time differences of two daughter cells from the same mother cells (Fig. 7) suggests the involvement of a probabilistic process that starts division. A Poissonian variation in a small number of molecules that determines growth and division might explain the origin of these non-genetic variations in cells.

2.3 Differential Analysis of Direct Descendant Cells with Identical Genetic Information and Experience

We next examined whether the characteristics of direct descendants of an isolated single cell could be inherited under isolated conditions using the on-chip single-cell cultivation/analysis system with optical trapping to maintain the isolated

condition of cells even after several generations of cell divisions [4, 6]. Figure 8 plots temporal variations in cell lengths of individuals and their descendants. Figure 8a shows schematics explaining the measured interdivision time and cell length. The four graphs (b–e) indicate growth and division patterns for four cells born from a single cell and isolated into the four chambers A–D in Fig. 4f.

Figure 9a also plots variations in interdivision times for consecutive generations of other isolated *E. coli* cells derived from a common ancestor. The four series of interdivision times varied around the overall mean value, 52 min (dashed line); the mean values of the four cell lines a, b, c, and d were 54, 51, 56 and 56 min, indicating rather small differences compared with the large variations in the interdivision times of consecutive generations. These results support the idea that interdivision time variations from generation to generation are dominated by fluctuations around the mean value, and this was evidence of a stabilized phenotype that was subsequently inherited. To explore this idea further, we examined the dependence of interdivision time on the interdivision time of the previous generation. We grouped all interdivision time data into four categories and calculated their distributions (Fig. 9b). A comparison of these distributions revealed that they were astonishingly similar, suggesting that there was no dependence on

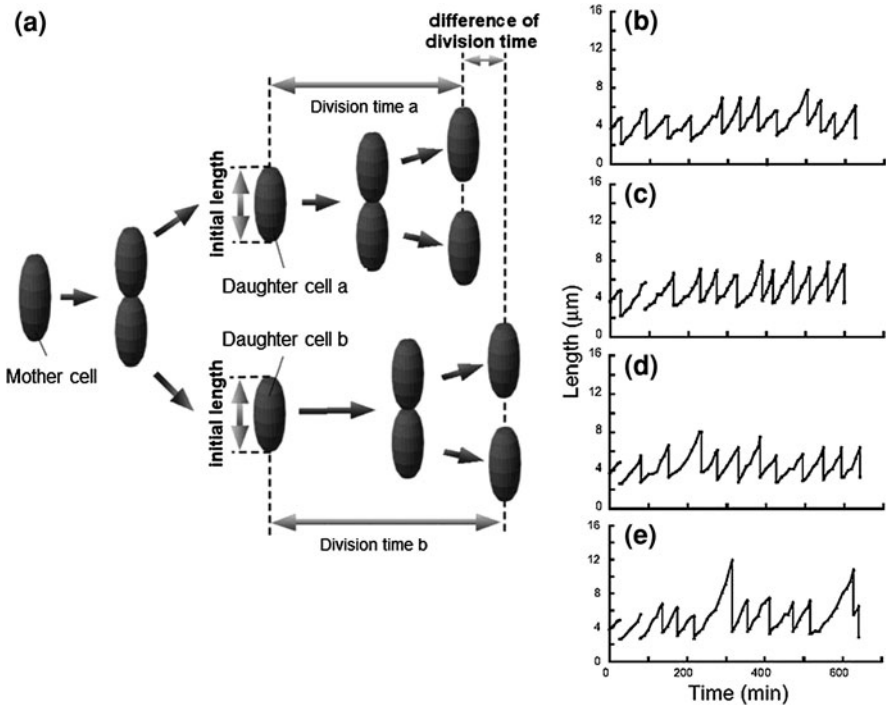

Fig. 8 Temporal variations in cell lengths of individual cells and their direct descendants

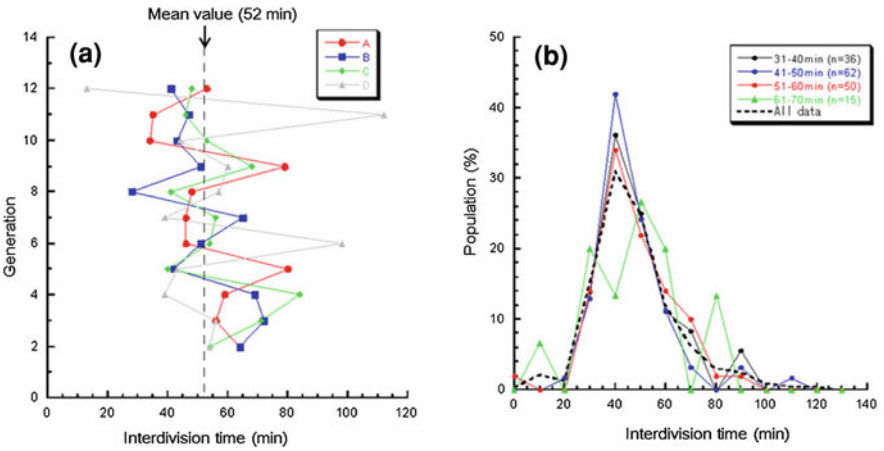

Mean values for 10 generations in each chamber

Chamber	A	B	C	D
Mean (min)	54	51	56	56

within (total mean time) ± 4 min

Fig. 9 Variations of interdivision time in direct descendant cells of *E. coli*

the previous generation. That is, there was no inheritance of interdivision time from one generation to the next.

2.4 *Adaptation Process for Sensor Proteins in Cells Caused by Environmental Changes*

We have modified the on-chip single-cell cultivation/analysis system to simultaneously measure the sensor-protein dynamics and motility of identical single cells for several generations [8]. This technique revealed the potential of combining the microfabrication technique (single-cell cultivation technique) and molecular biology (single-molecule observation).

Escherichiacoli cells are able to respond to changes in environmental chemoeffector concentrations through reversing their flagellar motors [50, 51]. Attractants (such as aspartate and serine) promote counterclockwise rotation of the flagella, resulting in a smooth swimming action, whereas repellents (such as phenol and Ni) promote clockwise rotation, resulting in tumbling. These responses are mediated by membrane-bound, methyl-accepting chemoreceptor proteins (MCPs). Immunoelectron microscopy revealed that MCP–CheW–CheA complexes are clustered in vivo, predominantly at the cell poles [52], and merely

weaker lateral clusters could be observed [53–55]. Polar localization changes have been expected according to environmental conditions, whereas no evidence concerning the dynamics of localization changes has been reported. Conventional group-based experiments do not allow the process of MCP clustering and the effect its change has on consecutive generations in individual cells, which is essential in estimating the changes occurring during the alternation of generations. To understand epigenetic processes such as adaptation and selection, both the protein dynamics and the cell dynamics of particular single cells should be observed continuously and simultaneously for several generations.

We used assayed intracellular proteins tagged with green fluorescent protein (GFP) to measure the localization dynamics of expressed proteins (Fig. 10).

We modified the shape of the microchambers into a wheel to measure the time course for motility (Fig. 11a). In the experiment, we first placed a single bacterium in the microchamber and isolated it in the wheel region so that it could swim along the track seal with the semipermeable membrane lid on the microchamber. Then, the bacterium running around the circle structure was continuously monitored by measuring the tumbling frequency and protein localization dynamics. When the cell divided into two daughter cells, one of these was picked up with the optical tweezers, transported to the axle area, and continuously confined in this region to stop it growing. The bacterium was chemically stimulated by changing the contents of the medium.

When the cultivation started, the tar localization ratio (filled squares) was 2.5 and the tumbling frequency (filled circles) was 0.5 (s^{-1}) (Fig. 11B-a and arrowhead 'a' in Fig. 11C). After the second cell division had occurred, a minimal medium containing 1 mM of aspartate was applied to the third-generation cell (135 min after microcultivation). After the attractant was added, tumbling frequency decreased immediately compared to the previous generation. Localization of the aspartate-sensitive sensor protein at two poles in *E. coli* (filled squares) also decreased quickly by half to 45 min following the change of medium (Fig. 11B-b, C-b). Finally, after 80 min of stimulation with the aspartate,

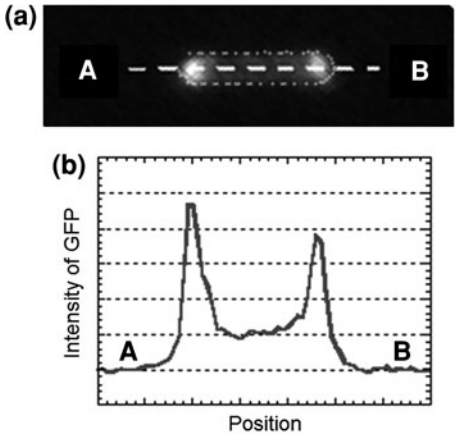

Fig. 10 MCP–GFP localization in *E. coli* cell. **a** Fluorescent micrograph of *E. coli*.**b** Intensity profile of MCP–GFP localization

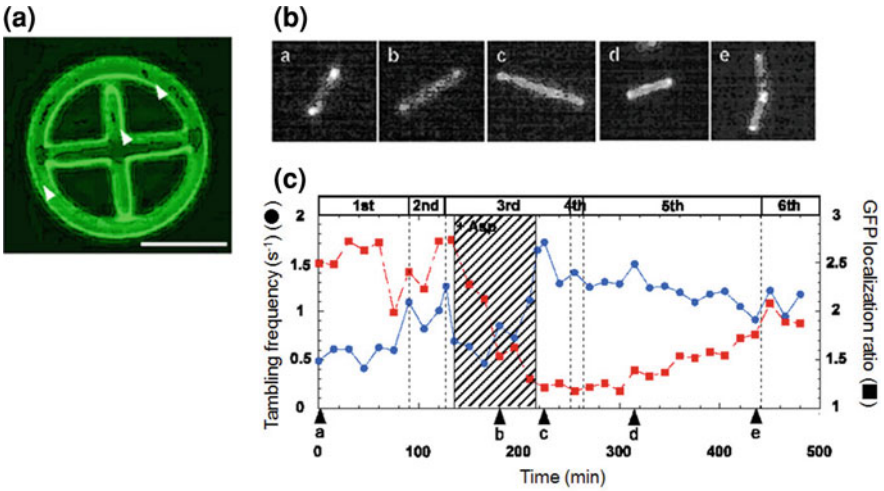

Fig. 11 Simultaneous observation of MCP–GFP localization and motility in identical *E. coli* cell for generations

the localized tar had diffused completely. Then, the aspartate was removed from the cultivation medium and the cells were cultivated further to enable the recovery of tar localization dynamics to be measured (Fig. 11B-c, C-c). After the first change of medium, it took more than three generations to recover the original pattern of tar localization (Fig. 11B-d, B-e, C-d, C-e). However, the frequency of tumbling remained higher than the former generations. This may indicate that tar localization requires more time to form than to diffuse. Such asymmetric reversibility in protein localization may contribute to cell phenomena being inherited in response to environmental changes [1, 4, 7, 56–66]. It also suggests the possibility that change in tar localization can be inherited by descendant cells and this can affect their motility and therefore their phenotype.

2.5 Epigenetic Inheritance of Elongated Phenotypes Between Generations Revealed by Individual-Cell-Based Direct Observation [67–76]

When implementing individual-cell-based measurements of epigenetic inheritance instead of group-based measurement, we developed an ‘on-chip individual-cell cultivation system’ [3, 4, 77]. This system enabled us to compare the phenotypes between generations and to examine the existence of phenotypic transmission at the individual cell level under stringently controlled conditions. We called this method a ‘differential individual-cell observation assay’. We measured the variations in quantitative traits at the individual cell level under uniform and isolated

conditions and found that the interdivision time, initial length, and final length varied at the individual cell level as much as 33, 26, and 26%, respectively [78].

This experiment reports the phenotypic dynamics involved in changing normal isolated cells into elongated ones, and the transmission of elongated phenotypes to descendants at the individual cell level, hence enabling epigenetic inheritance to be directly observed in *E. coli* using the differential individual-cell observation assay.

The *E. coli* strain EJ2848 (LacI3 ΔlacZ lacY+ΔfliC) [79] was used in this experiment. To simplify the model, we used a strain that lacks motility due to the deletion of flagellin. Cells were prepared by using M9 minimal medium (Qbiogene) supplemented with 0.2% (w/w) glucose and amino acids (MEM amino acids, Invitrogen). The cultivated cells were loaded and observed in the on-chip individual-cell cultivation system described in a previous report [78].

Figure 12a plots example growth and division dynamics of individual *E. coli* cells under uniform and isolated conditions. A single cell was first loaded in the on-chip individual-cell cultivation system and observed continuously (Fig. 12a). The cell exhibited normal growth and division patterns in the first and second

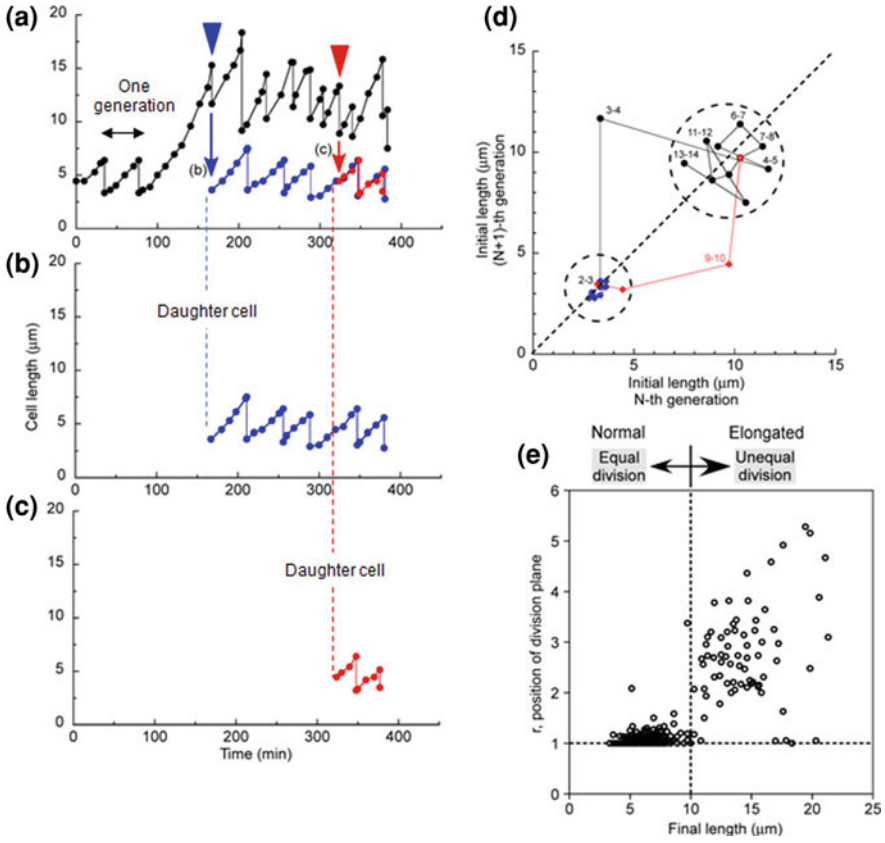

Fig. 12 Presence and inheritance of elongated phenotype under uniform conditions

generations and divided almost equally; hence, we randomly discarded one of the two daughter cells (closest to the exit). Despite the normal growth and division characteristics in the first and second generations, the cell in the third generation was extraordinarily elongated. A striking feature of the cell was that it divided unequally (Fig. 12a, arrowheads), thereby producing two daughter cells; one was elongated and the other was normal (Fig. 12a). Elongated daughter cells followed in the subsequent descendents, remaining elongated through repeated unequal cell divisions in most cell divisions. In other words, the cell transmitted its abnormally long cell length to its descendants. However, the normal daughter exhibited normal growth and division patterns and did not elongate in the following generations (Fig. 12b). The normal daughter cell born from the elongated cell had the same tendencies as those of typical normal cells. Just as in the third generation, the shorter of the two daughter cells in the ninth generation also demonstrated normal growth and division patterns (Fig. 12c). Therefore, it is conceivable that the shorter of the two daughters from the elongated cells possesses a normal phenotype.

The transmission of the elongated phenotype between generations can clearly be seen in the returning map of initial cell-length transitions (Fig. 12d). The converging dots indicate stable states in the transition. The initial cell-length transition for elongated lineage jumped from the normal cell-length area to the elongated cell-length area at the beginning of the fourth generation and stayed there throughout the following generations, whereas the shorter daughters' transitions were within the normal cell-length area. The clear distinction between the two transition areas hence indicates that the elongated cell transmitted a distinctive phenotype to one lineage of its descendants.

The presence of elongated cells was not restricted to this example. We found 5% of the normal-phenotype cells (12 out of 242) observed in the on-chip individual-cell cultivation system under the same conditions acquired elongated phenotypes.

The question is what is the mechanism responsible for passing on the elongated phenotype in one lineage of descendants? It should be noted that the evidence accrued from our results suggests the presence of elongated cells is not caused by the mutation of genetic information because one of the two daughters possessed normal cell characteristics, which should have had the same genetic information as the other elongated daughter cells. Otherwise, the normal of the two daughters would have elongated in the following generations if the elongation had been caused by mutation.

The repeated unequal divisions of elongated cells in Fig. 12a suggest that there is an intracellular mechanism that induces unequal cell divisions to elongate cells. Moreover, the mechanism for inducing unequal cell division should underlie the stable inheritance of the elongated phenotype in one lineage; unequal cell division produces a daughter cell with a long start cell, which would also attain a long cell by the next division, enabling it to divide unequally again. Repeating this process, a cell could stably transmit the elongated phenotype to the one lineage of descendants once they acquired a long cell.

The question arising from the above observations is whether there is a boundary for length that changes cell characteristics if variations exceed a certain length. We then examined the relationship between the final length and the position of the division plane (Fig. 12e). The position of the division plane, r, was defined by using the cell lengths of two daughter cells produced in the corresponding cell divisions as

$$r = \frac{(\text{Initial length of longer daughter cell})}{(\text{Initial length of shorter daughter cell})}. \quad (1)$$

Therefore, '$r = 1$' corresponds to equal cell division and '$r > 1$' corresponds to unequal cell division. Figure 12e shows that the position of the division plane was at an uneven point when the cell length was longer than 10 μm. The results clearly reveal that there is a boundary for cell length that affects division characteristics; cells shorter than 10 μm divide equally (normal phenotypes), while those longer than 10 μm divide unequally (elongated phenotypes). Hence, it is conceivable that a kind of geometric index, i.e., cell length, controls their phenotypic characteristics.

We next examined the division cycles of elongated cells. Figure 13a plots the interdivision time distributions for elongated and normal cells. 'Elongated cells' were defined as those whose final length was longer than 10 μm and those whose final length in the previous generation was also longer than 10 μm. Based on this definition, the interdivision time for generation in which a cell elongated extraordinarily from normal length (like the third generation in Fig. 12a) was not categorized as elongated in plotting the distribution. The average elongated-cell interdivision time was 25.9 ± 1.6 min, which was half that of normal cells (52.4 ± 1.1 min) and might be able to explain how the cell division process of both ends of the elongated cell proceeded independently. The coefficients of variance (CV) were 48 and 33% for the elongated and the normal, respectively. The distinct interdivision time distribution for elongated cells also confirms that they could easily be distinguished from normal cells. The characteristics of elongated cells cannot be explained by variations in normal cells. We thus regarded elongated and normal cells to be different phenotypes.

The next question is how does an elongated cell achieve a short interdivision time? Figure 13b shows an alternative formation for the division plane at opposite poles between neighboring generations. Image 1 shows an elongated cell emerging in the fourth generation from a normal phenotype before the division plane is formed. A visible division plane was then formed near the lower end as can be seen from Image 2 (fourth generation). After cell division, the longest daughter cell was selected and observed thereafter. We found a division plane was formed in the next generation near the opposite end of the cell (Image 3, fifth generation). Although the cell divided equally and produced two elongated daughters in the sixth generation, the division ended in the following two generations (seventh and eighth) exhibiting the same behavior as in the fourth and fifth generations, i.e., division planes were generated on opposite sides (Images 4 and 5).

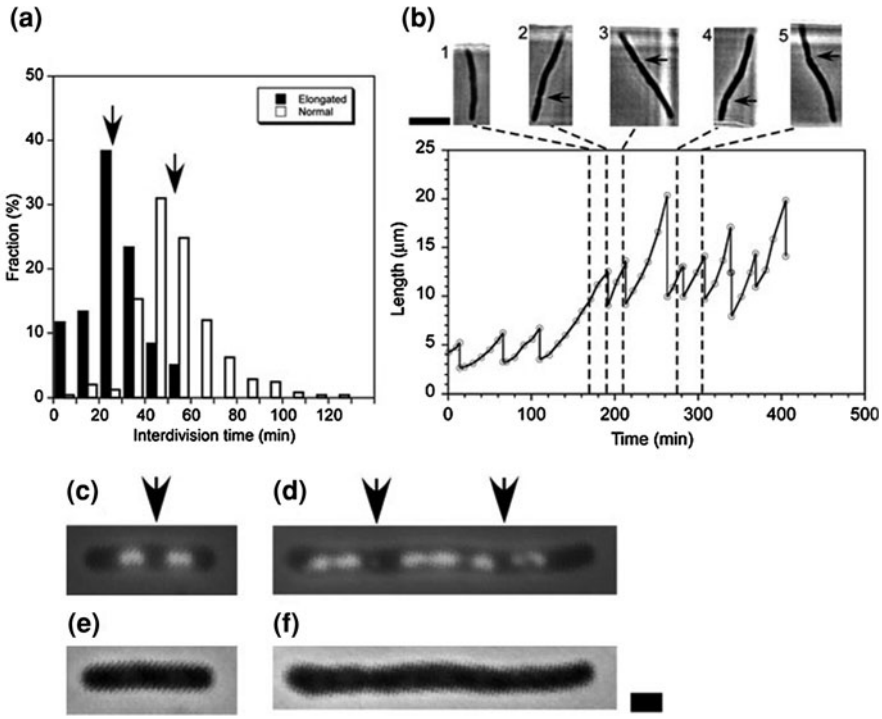

Fig. 13 Short interdivision time for elongated cell. *Bar* 1 μm

The fact that the positions of division planes in consecutive generations (fourth–fifth and seventh–eighth) were opposite indicates that two division mechanisms operate simultaneously in an elongated cell near both ends. The half interdivision time of elongated cells can be explained by two division planes simultaneously and independently working near both ends in elongated cells, each of which works at approximately the same interval as interdivision in the normal phenotype.

The question then is what intracellular mechanism is responsible for the observed unequal cell divisions in elongated cells? It has been suggested that two mechanisms in *E. coli*, nucleoid occlusion and the Min system, determine the position of the division plane. Nucleoid occlusion is the mechanism where the assembly of the FtsZ ring, which determines the position of the final cell division plane, is inhibited within the close vicinities of nucleoids [80, 81]. The Min system, on the other hand, is comprised of three proteins, MinC, MinD, and MinE, which dynamically interact with one another and exhibit rapid pole-to-pole oscillations [82–92]. MinC and MinD form an inhibitory complex to form Z rings [85–87]; Z-ring formation has been proposed to be directed to positions where concentrations of the MinCD complex are low on average in oscillations [89, 91, 92]. To examine the relevance of observed unequal cell divisions to the proposed mechanisms responsible for the position of the division plane,

we visualized the position of nucleoids in elongated cells by 4′,6-diamidino-2-phenylindole dihydrochloride hydrate (DAPI) fluorescence using Hiraga's method [93] (Fig. 13c, d). A normal-sized cell reaching the mean division length possessed two segregated nucleoids with a space in the middle as seen in Fig. 13c (phase-contrast image for reference in Fig. 13e). MinCD concentration should be low in the middle and high at the poles [89, 91, 92], leading to Z-ring formation in the middle. However, an elongated cell possessed multiple nucleoids with spaces between them as can be seen from Fig. 13d (phase-contrast image for reference in Fig. 13f). There are numerous positions where constrictions can occur in this elongated cell according to the nucleoid occlusion model. However, MinCDE oscillations are known to achieve 'doubled' patterns in an elongated cell [85, 86, 88], which has been proposed to inhibit Z-ring formation both around the midplane and at the poles. Consequently, the cell divisions in elongated cells of this size should only occur at the uneven nucleoid gap positions (Fig. 13d, arrows).

Although the presence of unequal cell divisions in elongated cells is understandable from the combined views of nucleoid occlusion and Min oscillation, it is still unclear what determines the cell-length boundary, 10 μm, between the equal and unequal cell divisions shown in Fig. 12e. We therefore calculated the oscillation dynamics of the MinCD complex and MinE at various cell lengths according to Huang's model (Fig. 14) [92]. Figure 14a–e are micrographs of the time course change in the concentration of MinD at the cell membrane along the long axis of the cell, indicating that the number of oscillations doubles when the cell length is longer than 8 μm. The single-cycle averages for MinD concentration at the membrane in Fig. 14a–e also reveal the concentration of MinD at the midplane becomes highest for all positions when the cell length is longer than 8 μm. The MinD concentration at the midplane relative to the overall averages is plotted in Fig. 14f. The results indicate a drastic increase in MinD concentration at the midplane when the oscillation doubles, which suggests that the cell-length boundary between the single and double oscillations of Min proteins determines the cell-length boundary between equal and unequal cell divisions in Fig. 12e.

On the basis of the results in Fig. 14f, FtsZ should be unable to form a ring at the midplane in cells with lengths longer than 8 μm. Therefore, FtsZ would inevitably form rings at uneven positions in these long cells, which would lead to unequal cell divisions. The formation of FtsZ rings lies at the heart of the process of division at the membrane [94]. In previous studies, the time between when cell division was initiated by the polymerization of FtsZ and the appearance of constriction visualized by electron microscopy was found to be approximately 20 min [95]. Under the conditions in our experiment, the average time to double cell length was 52 min (Fig. 13a); hence, the expected division cell-length for a cell whose Z-ring formation was initiated at a cell length of 8 μm can be calculated as $8\ \mu m \times 2^{20/52} = 10.4\ \mu m$. This calculation suggests that the boundary for final length that separates equal and unequal cell divisions should be 10.4 μm, which matches our experimental results in Fig. 12e. All these results indicate that it is highly probable that Min oscillations determine the observed cell-length boundary between equal and unequal cell divisions.

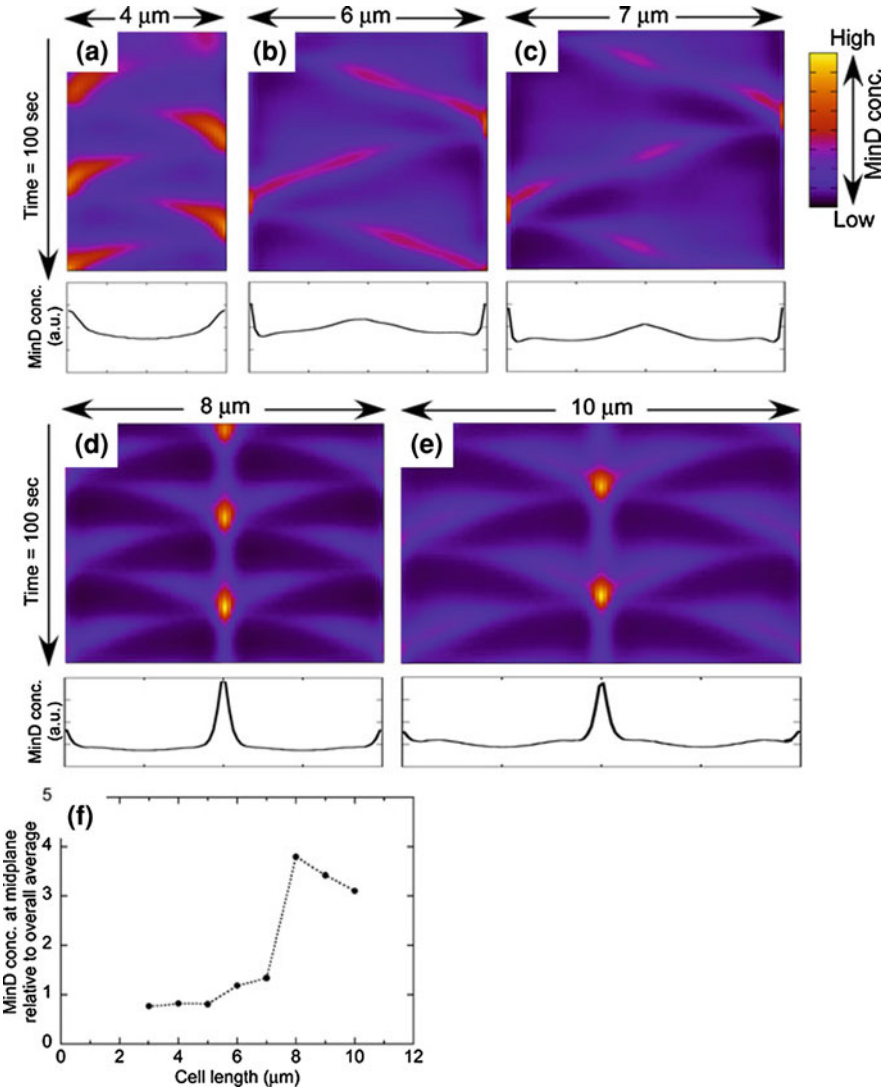

Fig. 14 Simulated MinD dynamics within cells with various cell lengths

It is still unclear at this point how a cell acquires length. We previously reported that the length distributions for the division of genetically identical cells in the same environment had variations of 26% (CV) [78]. The large variations in cell-length distributions reflect uncertainty about whether genetically identical cells can generate the same length when the environmental conditions are the same. In other words, the intracellular mechanism inevitably includes stochasticity, which causes variations in the length of divided cells. Therefore, extraordinarily elongated cells with final lengths longer than 10 μm can occur with a certain

probability based on intracellular stochasticity; this occurred with 5% probability under our test conditions.

The fact that elongated cells divide unequally would enable the elongated phenotype to be inherited in one lineage. Unequal cell division produces longer and shorter daughter cells. The longer daughter cell with a long starting cell length can easily exceed the boundary cell length. Consequently, the next division also becomes unequal. Repeating this process, a cell will eventually transmits its longer length to one of its descendant once it has acquired that length. Geometry, i.e., cell length in this inheritance mechanism, plays a key role in enabling the phenotypic characteristics to be inherited between generations without any consideration given to genetic modifications.

The mechanisms for cellular epigenetic inheritance have mainly been studied to reveal the gene regulatory network to achieve multistability [75, 76, 96, 97] to the best of our knowledge. The roles of chromatin, DNA methylation, and acetylation also relate to gene regulation [74, 98–100]. However, the epigenetic inheritance discussed in this chapter occurred once a cell reached a certain cell length; it was independent of the gene regulatory network. Therefore, our results suggest the inheritance of geometric information, such as cell shape, is significant in epigenetic inheritance.

3 Conclusion

We developed and used a series of new methods for understanding the meaning of genetic and epigenetic information in a life system from a 'temporal' or 'algebraic' viewpoint by exploiting microstructures fabricated on a chip. The most important contribution of this study was to be able to reconstruct the concept of a cell regulatory network from the 'local' (molecules expressed at certain times and places) to the 'global' (the cell as a viable, functioning system). Knowledge of epigenetic information, which we can control and change during cell lives, complements the genetic variety, and these two kinds are indispensable for living organisms. This new kind of knowledge has the potential to be the basis of cell-based biological and medical fields like those involving cell-based drug screening and the regeneration of organs from stem cells.

Acknowledgments The author acknowledges the assistance of all members of Yasuda Lab. Financial support, in part from the Japan Science and Technology Agency (JST) and from Grants-in-Aids for Scientific Research from the Ministry of Education, Culture, Sports, Science and Technology of the Japanese government, is gratefully appreciated.

References

1. Spudich JL, Koshland DE Jr (1976) Non-genetic individuality: chance in the single cell. Nature 262:467–471
2. Yasuda K (2000) Non-destructive, non-contact handling method for biomaterials in micro-chamber by ultrasound. Sens Actuators B Chem 64:128–135

3. Inoue I, Wakamoto Y, Moriguchi H, Okano K, Yasuda K (2001) On-chip culture system for observation of isolated individual cells. Lab Chip 1:50–55
4. Wakamoto Y, Inoue I, Moriguchi H, Yasuda K (2001) Analysis of single-cell differences using on-chip microculture system and optical trapping. Fresenius J Anal Chem 371:276–281
5. Inoue I, Wakamoto Y, Yasuda K (2001) Non-genetic variability of division cycle and growth of isolated individual cells in on-chip culture system. Proc Jpn Acad 77B:145–150
6. Wakamoto Y, Umehara S, Matsumura K, Inoue I, Yasuda K (2003) Development of non-destructive, non-contact single-cell based differential cell assay using on-chip microcultivation and optical tweezers. Sens Actuators B Chem 96:693–700
7. Umehara S, Wakamoto Y, Inoue I, Yasuda K (2003) On-chip single-cell microcultivation assay for monitoring environmental effects on isolated cells. Biochem Biophys Res Commun 305:534–540
8. Inoue I, Shiomi D, Kawagishi I, Yasuda K (2004) Simultaneous measurement of sensor-protein dynamics and motility of a single cell by on-chip microcultivation system. J Nanobiotechnology 2:4
9. Takahashi K, Matsumura K, Yasuda K (2003) On-chip microcultivation chamber for swimming cells using visualized poly(dimetylsiloxane) valve. Jpn J Appl Phys 42:L1104–L1107
10. Hattori A, Umehara S, Wakamoto Y, Yasuda K (2003) Measurement of incident angle dependence of swimming bacterium reflection using on-chip single-cell cultivation assay. Jpn J Appl Phys 42:L873–L875
11. Matsumura K, Yagi T, Yasuda K (2003) Role of timer and sizer in regulation of *Chlamydomonas* cell cycle. Biochem Biophys Res Commun 306:1042–1049
12. Matsumura K, Yagi T, Yasuda K (2003) Differential analysis of cell cycle stability in *Chlamydomonas* using on-chip single-cell cultivation system. Jpn J Appl Phys 42:L784–L787
13. Moriguchi H, Wakamoto Y, Sugio Y, Takahashi K, Inoue I, Yasuda Y (2002) An agar-microchamber cell-cultivation system: flexible change of microchamber shapes during cultivation by photo-thermal etching. Lab Chip 2:125–30
14. Hattori A, Moriguchi H, Ishiwata S, Yasuda K (2004) A 1480-nm/1064-nm dual wavelength photo-thermal etching system for non-contact three-dimensional microstructure generation into agar microculture chip. Sens Actuators B Chem 100:455–462
15. Sugio Y, Kojima K, Moriguchi H, Takahashi K, Kaneko T, Yasuda K (2004) An agar-based on-chip neural-cell cultivation system for stepwise control of network pattern generation during cultivation. Sens Actuators B Chem 99:156–162
16. Moriguchi H, Takahashi K, Sugio Y, Wakamoto Y, Inoue I, Jimbo Y, Yasuda K (2003) On chip neural cell cultivation using agarose-microchamber array constructed by photo-thermal etching method. Electr Eng Jpn 146:37–42
17. Suzuki I, Sugio Y, Jimbo Y, Yasuda K (2004) Individual-cell-based electrophysiological measurement of a topographically controlled neuronal network pattern using agarose architecture with a multi-electrode array. Jpn J Appl Phys 43(3B):L403–L406
18. Suzuki I, Sugio Y, Jimbo Y, Yasuda K (2004) Modification of a neuronal network direction using stepwise photo-thermal etching of an agarose architecture. J Nanobiotechnology 2:7
19. Kojima K, Moriguchi H, Hattori A, Kaneko T, Yasuda K (2003) Two-dimensional network formation of cardiac myocytes in agar microculture chip with 1480-nm infrared laser photo-thermal etching. Lab Chip 3:299–303
20. Kojima K, Kaneko T, Yasuda K (2006) Role of the community effect of cardiomyocyte in the entrainment and reestablishment of stable beating rhythms. Biochem Biophys Res Commun 351:209–215
21. Yasuda K, Okano K, Ishiwata S (2000) Focal extraction of surface-bound DNA from a microchip using photo-thermal denaturation. Biotechniques 28:1006–1011
22. Gally DL, Bogan JA, Eisenstein BI, Blomfield IC (1993) Environmental regulation of the fim switch controlling type 1 fimbrial phase variation in *Escherichia coli* K-12: effects of temperature and media. J Bacteriol 175:6186–6193

23. Ko MS, Nakauchi H, Takahashi N (1990) The dose dependence of glucocorticoid-inducible gene expression results from changes in the number of transcriptionally active templates. EMBO J 9:2835–2842
24. Msadek T (1999) When the going gets tough: survival strategies and environmental signaling networks in *Bacillus subtilis*. Trends Microbiol 7:201–207
25. Schwan WR, Seifert HS, Duncan JL (1992) Growth conditions mediate differential transcription of fim genes involved in phase variation of type 1 pili. J Bacteriol 174: 2367–2375
26. Shapiro JA (1995) The significances of bacterial colony patterns. Bioessays 17:597–607
27. Shapiro JA (1998) Thinking about bacterial populations as multicellular organisms. Annu Rev Microbiol 52:81–104
28. Shapiro JA, Hsu C (1989) *Escherichia coli* K-12 cell–cell interactions seen by time-lapse video. J Bacteriol 171:5963–5974
29. Arkin A, Ross J, McAdams HH (1998) Stochastic kinetic analysis of developmental pathway bifurcation in phage lambda-infected *Escherichia coli* cells. Genetics 149:1633–1648
30. Kepler TB, Elston TC (2001) Stochasticity in transcriptional regulation: origins, consequences, and mathematical representations. Biophys J 81:3116–3136
31. Kierzek AM, Zaim J, Zielenkiewicz P (2001) The effect of transcription and translation initiation frequencies on the stochastic fluctuations in prokaryotic gene expression. J Biol Chem 276:8165–8172
32. Levin MD, Morton-Firth CJ, Abouhamad WN, Bourret RB, Bray D (1998) Origins of individual swimming behavior in bacteria. Biophys J 74:175–181
33. McAdams HH, Arkin A (1997) Stochastic mechanisms in gene expression. Proc Natl Acad Sci USA 94:814–819
34. Thattai M, van Oudenaarden A (2001) Intrinsic noise in gene regulatory networks. Proc Natl Acad Sci USA 98:8614–8619
35. Blake WJ, Kaern M, Cantor CR, Collins JJ (2003) Noise in eukaryotic gene expression. Nature 422:633–637
36. Elowitz MB, Levine AJ, Siggia ED, Swain PS (2002) Stochastic gene expression in a single cell. Science 297:1183–1186
37. Ozbudak EM, Thattai M, Kurtser I, Grossman AD, van Oudenaarden A (2002) Regulation of noise in the expression of a single gene. Nat Genet 31:69–73
38. Rao CV, Wolf DM, Arkin AP (2002) Control, exploitation and tolerance of intracellular noise. Nature 420:231–237
39. Åkerlund T, Nordström K, Bernander R (1995) Analysis of cell size and DNA content in exponentially growing and stationary-phase batch cultures of *Escherichia coli*. J Bacteriol 177:6791–6797
40. Donachie DD, Begg KJ (1996) 'Division potential' in *Escherichia coli*. J Bacteriol 178:5971–5976
41. Elowitz MB, Leibler S (2000) A synthetic oscillatory network of transcriptional regulators. Science 403:335–338
42. Gardner TS, Cantor CR, Collins JJ (2000) Construction of a genetic toggle switch in *Escherichia coli*. Science 403:339–342
43. Panda AK, Khan RH, Appa Rao KBC, Totey SM(1999) Kinetics of inclusion body production in batch and high cell density fed-batch culture of *Escherichia coli* expressing ovine growth hormone. J Biotech 75:161–172
44. Ashkin A, Dziedzic JM, Bjorkholm JE, Chu S (1986) Observation of a single-beam gradient force optical trap for dielectric particles. Opt Lett 11:288–290
45. Ashkin A, Dziedzic JM, Yamane T (1987) Optical trapping and manipulation of single cells using infrared laser beams. Nature 330:769–771
46. Ashkin A, Dziedzic JM (1989) Internal cell manipulation using infrared laser traps. Proc Natl Acad Sci USA 86:7914–7918

47. Ashkin A, Schutze K, Dziedzic JM, Euteneuer U, Schliwa M (1990) Force generation of organelle transport measured in vivo by an infrared laser trap. Nature 348:346–348
48. Wright W, Sonek GJ, Tadir Y, Berns MW (1990) Laser trapping in cell biology. IEEE J Quantum Electron 26:2148–2157
49. Svoboda K, Block SM (1994) Biological applications of optical forces. Annu Rev Biophys Biomol Struct 23:247–285
50. Levit MN, Liu Y, Stock JB (1998) Stimulus response coupling in bacterial chemotaxis: receptor dimers in signalling arrays. Mol Microbiol 30:459–466
51. Manson MD, Armitage JP, Hoch JA, Macnab RM (1998) Bacterial locomotion and signal transduction. J Bacteriol 180:1009–1022
52. Maddock JR, Shapiro L (1993) Polar location of the chemoreceptor complex in the *Escherichia coli* cell. Science 259:1717–1723
53. Lybarger SR, Maddock JR (1999) Clustering of the chemoreceptor complex in *Escherichia coli* is independent of the methyltransferase CheR and the methylesterase CheB. J Bacteriol 181:5527–5529
54. Skidmore JM, Ellefson DD, McNamara BP, Couto MM, Wolfe AJ, Maddock JR (2000) Polar clustering of the chemoreceptor complex in *Escherichia coli* occurs in the absence of complete CheA function. J Bacteriol 182:967–973
55. Umehara S, Inoue I, Wakamoto Y, Yasuda K (2007) Origin of individuality of two daughter cells during the division process examined by the simultaneous measurement of growth and swimming property using an on-chip single-cell cultivation system. Biophys J 93(3):1061–1067
56. Stock, JB, Surette MG (1996) Chemotaxis. In Neidhardt FC, Curtiss R III, Ingraham JL, Lin ECC, Low KB, Magasanik B, Rfznikopp WS, Riley M, Schaechter M, Umbarger HE (eds) *Escherichia coli* and *Salmonella*: cellular and molecular biology, 2nd edn. ASM, Washington, pp 1103–1129
57. Magariyama, Y, Sugiyama S, Muramoto K, Kawagishi I, Imae Y, Kudo S (1995) Simultaneous measurement of bacterial flagellar rotation rate and swimming speed. Biophys J 69:2154–2162
58. Amsler CD, Cho M, Matsumura P (1993) Multiple factors underlying the maximum motility of *Escherichia coli* as cultures enter post-exponential growth. J Bacteriol 175:6238–6244
59. Pruss BM, Matsumura P (1996) A regulator of the flagellar regulon of *Escherichia coli*, *flhD*, also affects cell division. J Bacteriol 178:668–674
60. Aizawa SI, Kubori T (1998) Bacterial flagellation and cell division. Genes Cells 3:625–634
61. Hattori A, Umehara S, Wakamoto Y, Yasuda K (2003) Measurement of incident angle dependence of swimming bacterium reflection using on-chip single-cell cultivation assay. Jpn J Appl Phys 2 42:L873–L875
62. Umehara S, Hattori A, Wakamoto Y, Yasuda K (2004) Simultaneous measurement of growth and movement of cells exploiting on-chip single-cell cultivation assay. Jpn J Appl Phys 1 43:1214–1217
63. Wakamoto Y, Umehara S, Matsumura K, Inoue I, Yasuda K (2003) Development of non-destructive, non-contact single-cell based differential cell assay using on-chip microcultivation and optical tweezers. Sens Actuators B Chem 96:693–700
64. Mesibov R, Adler J (1972) Chemotaxis toward amino acids in *Escherichia coli*. J Bacteriol 112:315–326
65. Alon U, Camarena L, Surette MG, Aguera y Arcas B, Liu Y, Leibler S, Stock JB (1998) Response regulator output in bacterial chemotaxis. EMBO J 17:4238–4248
66. Maki N, Gestwicki JE, Lake EM, Kiessling LL, Adler J (2000) Motility and chemotaxis of filamentous cells of *Escherichia coli*. J Bacteriol 182:4337–4342
67. Wakamoto Y, Yasuda K (2006) Epigenetic inheritance of elongated phenotypes between generations revealed by individual-cell-based direct observation. Meas Sci Technol 17:3171–3177

68. Cohn M, Horibata K (1959) Physiology of the inhibition by glucose of the induced synthesis of the β-galactoside-enzyme system of *Escherichia Coli*. J Bacteriol 78:601–12
69. Pal C, Miklos I (1999) Epigenetic inheritance, genetic assimilation and speciation. J Theor Biol 200:19–37
70. Jablonka E, Lachmann M, Lamb MJ (1992) Evidence, mechanisms and models of the inheritance of acquired characters. J Theor Biol 158:245–268
71. Jablonka E, Lamb MJ (1998) Epigenetic inheritance in evolution. J Evol Biol 11:159–183
72. Mameli M (2004) Nongenetic selection and nongenetic inheritance. Br J Philos Sci 55:35–71
73. Solomon F (1981) Specification of cell morphology by endogenous determinants. J Cell Biol 90:547–553
74. Casadesus J, D'Ari R (2002) Memory in bacteria and phage. Bioessays 24:512–518
75. Gardner TS, Cantor CR, Collins JJ (2000) Construction of a genetic toggle switch in *Escherichia coli*. Nature 403:339–42
76. Ozbudak EM, Thattai M, Lim HN, Shraiman BI, van Oudenaarden A (2004) Multistability in the lactose utilization network of *Escherichia coli*. Nature 427:737–40
77. Wakamoto Y, Umehara S, Matsumura K, Inoue I, Yasuda K (2003) Development of non-destructive, non-contact single-cell based differential cell assay using on-chip microcultivation and optical tweezers. Sens Actuators B Chem 96:693–700
78. Wakamoto Y, Ramsden J, Yasuda K (2005) Single-cell growth and division dynamics showing epigenetic correlations. Analyst 130:311–317
79. Mukaihara T, Enomoto M (1997) Deletion formation between the two Salmonella typhimurium flagellin genes encoded on the mini F plasmid: *Escherichia coli* ssb alleles enhance deletion rates and change hot-spot preference for deletion endpoints. Genetics 145:563–72
80. Yu XC, Margolin W (1999) FtsZ ring clusters in min and partition mutants: role of both the Min system and the nucleoid in regulating FtsZ ring localization. Mol Microbiol 32:315–326
81. Woldringh CL, Mulder E, Valkenburg JA, Wientjes FB, Zaritsky A, Nanninga N (1990) Role of the nucleoid in toporegulation of division. Res Microbiol 141:39–49
82. de Boer PA, Crossley RE, Rothfield LI (1989) A division inhibitor and a topological specificity factor coded for by the minicell locus determine proper placement of the division septum in *E. coli*. Cell 56:641–9
83. de Boer PA, Crossley RE, Rothfield LI (1992) Roles of MinC and MinD in the site-specific septation block mediated by the MinCDE system of *Escherichia coli*. J Bacteriol 174:63–70
84. Bi E, Lutkenhaus J (1993) Cell division inhibitors SulA and minCD prevent formation of the FtsZ ring. J Bacteriol 175:1118–25
85. Raskin DM, de Boer PA (1999) Rapid pole-to-pole oscillation of a protein required for directing division to the middle of *Escherichia coli*. Proc Natl Acad Sci USA 96:4971–4976
86. Raskin DM, de Boer PA (1999) MinDE-dependent pole-to-pole oscillation of division inhibitor MinC in *Escherichia coli*. J Bacteriol 181:6419–24
87. Hu Z, Lutkenhaus J (1999) Topological regulation of cell division in *Escherichia coli* involves rapid pole to pole oscillation of the division inhibitor MinC under the control of MinD and MinE. Mol Microbiol 34:82–90
88. Fu X, Shih YL, Zhang Y, Rothfield LI (2001) The MinE ring required for proper placement of the … its cellular location during the *Escherichia coli* division cycle. Proc Natl Acad Sci USA 98:980–985
89. Meinhardt H, de Boer PA (2001) Pattern formation in *Escherichia coli*: a model for the pole-to-pole oscillations of Min proteins and the localization of the division site. Proc Natl Acad Sci USA 98:14202–14207
90. Pichoff S, Lutkenhaus J (2001) *Escherichia coli* division inhibitor MinCD blocks septation by preventing Z-ring formation. J Bacteriol 183:6630–6635
91. Howard M, Rutenberg AD, de Vet S (2001) Dynamic compartmentalization of bacteria: accurate division in *E. coli*. Phys Rev Lett 87:278102

92. Huang KC, Meir Y, Wingreen NS (2003) Dynamic structures in *Escherichia coli*: spontaneous formation of MinE rings and MinD polar zones. Proc Natl Acad Sci USA 100:12724–12728
93. Hiraga S, Niki H, Ogura T, Ichinose C, Mori H, Ezaki B, Jaffe A (1989) Chromosome partitioning in *Escherichia coli*: novel mutants producing anucleate cells. J Bacteriol 171:1496–1505
94. Aarsman, ME, Piette A, Fraipont C, Vinkenvleugel TM, Nguyen-Disteche M, den Blaauwen T (2005) Maturation of the *Escherichia coli* divisome occurs in two steps. Mol Microbiol 55:1631–1645
95. Den Blaauwen T, Buddelmeijer N, Aarsman ME, Hameete CM, Nanninga N (1999) Timing of FtsZ assembly in *Escherichia coli*. J Bacteriol 181:5167–5175
96. Thomas R (1998) Laws for the dynamics of regulatory circuits. Int J Dev Biol 42:479–485
97. Thomas R, Kaufman M (2001) Multistationarity, the basis of cell differentiation and memory. II. Logical analysis of regulatory networks in terms of feedback circuits. Chaos 11:180–195
98. Hernday AD, Braaten BA, Low DA (2003) The mechanism by which DNA adenine methylase and PapI activate the pap epigenetic switch. Mol Cell 12:947–957
99. van der Woude M, Braaten B, Low D (1996) Epigenetic phase variation of the pap operon in *Escherichia coli*. Trends Microbiol 4:5–9
100. McNairn AJ, Gilbert DM (2003) Epigenomic replication: linking epigenetics to DNA replication. Bioessays 25:647–656